Anomalous Nuclear Quantum Effects in Ice

B. Pamuk,[1] J. M. Soler,[2] R. Ramírez,[3] C. P. Herrero,[3] P. W. Stephens,[1,4] P. B. Allen,[1] and M.-V. Fernández-Serra[1,*]

[1]*Department of Physics and Astronomy, Stony Brook University, Stony Brook, New York 11794-3800, USA*
[2]*Dep. de Física de la Materia Condensada, Universidad Autónoma de Madrid, 28049 Madrid, Spain*
[3]*Instituto de Ciencia de Materiales, Consejo Superior de Investigaciones Cientificas (CSIC), Campus de Cantoblanco, 28049 Madrid, Spain*
[4]*Photon Sciences Directorate, Brookhaven National Lab, Upton, New York 11973, USA*

(Received 18 November 2011; published 9 May 2012)

One striking anomaly of water ice has been largely neglected and never explained. Replacing hydrogen (^{1}H) by deuterium (^{2}H) causes ice to expand, whereas the normal isotope effect is volume contraction with increased mass. Furthermore, the anomaly increases with temperature T, even though a normal isotope shift should decrease with T and vanish when T is high enough to use classical nuclear motions. In this study, we show that these effects are very well described by *ab initio* density-functional theory. Our theoretical modeling explains these anomalies, and allows us to predict and to experimentally confirm a counter effect, namely, that replacement of ^{16}O by ^{18}O causes a normal lattice contraction.

DOI: 10.1103/PhysRevLett.108.193003 PACS numbers: 31.15.A−, 31.70.Ks, 65.40.De, 71.15.Pd

Numerous recent studies [1–7] address the contribution of zero-point nuclear quantum effects to the structures of ice and water. The issue is delicate, because of the peculiar electrostatic-covalent nature [8] of the hydrogen bond (Hbond) in water. It is well known that hydrogen bonded materials show an anticorrelation [9] effect between the OH covalent bond and the OH-O Hbond. As the OH-O distance diminishes, the OH covalent bond weakens (its length increases and vibrational frequency diminishes [10,11]) while the OH-O Hbond does the opposite. Closely related is the surprising expansion of the ice (Ih) crystal [12,13] when H_2O is replaced by D_2O. A similar effect is observed in water, where the molecular volume of H_2O is smaller than that of D_2O [14] at all temperatures. Zero-point expansion of crystal lattices is a well understood phenomenon, and is almost always greatest for the lightest isotopes. For example, the volume of ^{20}Ne expands by 0.6% with respect to ^{22}Ne at $T = 0$ [15]. This normal isotope effect corresponds to a $\sim 12\%$ zero-point expansion of ^{20}Ne relative to a hypothetical ''classical'' or ''frozen'' lattice [16,17]. Since H_2O and Ne have similar molecular masses, one might expect similar effects. However, the volume of H_2O at $T = 0$ is $\sim$0.1% smaller than that of D_2O [12,13]. It has rarely been mentioned in the literature that this is opposite to the usual behavior, and no explanation has been offered.

In this Letter, we explain this effect as an interesting coupling between quantum nuclear motion and hydrogen bonding, that may be relevant also to the structure of liquid water. Our analysis shows that, despite the anomalous isotope effect, quantum ice actually has a volume 1% larger than it would have with classical nuclei. The effects are smaller than in Ne mostly because of delicate cancellations. We exploit these cancellations to make critical comparisons of (i) quasiharmonic theory versus fully anharmonic path-integral molecular dynamics (PIMD), (ii) *ab initio* forces versus flexible and polarizable empirical force fields (EFF), and (iii) various flavors of *ab initio* density-functional theory (DFT) exchange and correlation (XC) density functionals (DF) with and without inclusion of van der Waals (vdW) interactions. We find (i) quasiharmonic theory is satisfactory for this problem, (ii) present state of the art EFFs are not good enough to describe nuclear quantum effects in water, and (iii) all the DFs considered describe qualitatively the anomalous effects, although some versions perform better than others.

Within the volume-dependent quasiharmonic approximation (QHA), the equilibrium volume $V(T)$ is obtained by minimizing at each T the Helmholtz free energy $F(V, T)$ [18,19]

$$F(V,T) = E_0(V) + \sum_k \left[\frac{\hbar\omega_k(V)}{2} + k_B T \ln(1 - e^{-\hbar\omega_k(V)/k_B T}) \right], \tag{1}$$

where $E_0(V)$ is the energy for classical ($T = 0$ or frozen) nuclei, at the relaxed atomic coordinates for each volume. ω_k are the phonon frequencies, with k combining the branch index and the phonon wave vector within the Brillouin zone. Their volume dependence is linearized as

$$\omega_k(V) = \omega_k(V_0)\left[1 - \frac{(V - V_0)}{V_0}\gamma_k \right], \tag{2}$$

where $\gamma_k = -(V_0/\omega_k)(\partial\omega_k/\partial V)_{V_0}$ is the Grüneisen parameter of the mode, and V_0 is the equilibrium volume of $E_0(V)$. $\omega_k(V_0)$ and $\gamma_k(V_0)$ are obtained by diagonalizing the dynamical matrix, computed by finite differences from the atomic forces in a $(3 \times 3 \times 3)$ supercell, at two volumes slightly below and above V_0. As shown in the supplementary material [20], this linearization is an excellent

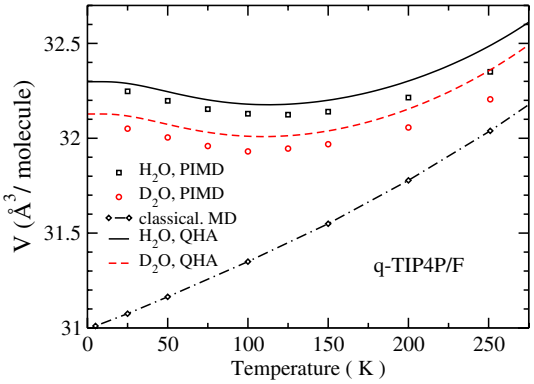

FIG. 1 (color online). Volume per molecule for different isotopes calculated using the q-TIP4P/F force field both with PIMD [6] simulations and the QHA.

approximation to the full QHA, in which the frequencies are calculated at each volume. It can be easily shown [20] that at $T = 0$ the quasiharmonic volume shift with respect to the frozen lattice is isotope dependent, and proportional to the average $\langle \gamma_k \omega_k \rangle$. For increasing temperature, quantum effects become less relevant, and the shift converges to the classical result, where the change in volume is $\propto T$ and isotope independent. Therefore, for high enough T, the differences between isotopes must vanish.

Anharmonic effects, beyond the QHA, could change the $V(T)$ curves calculated with this method. However, experimental Raman spectra of ice Ih, as a function of pressure and temperature [10,21,22] show a relatively temperature-insensitive stretching band, with $\partial\omega/\partial T < 0.6$ cm^{-1}K^{-1}. Such a small anharmonicity should not modify the QHA results.

To test the validity of the QHA in ice Ih, Fig. 1 compares the QHA result for $V(T)$ with our fully anharmonic PIMD simulations [6], using the q-TIP4P/F force field [2] in both cases. Differences between the QHA and PIMD increase with temperature, but their overall agreement is satisfactory. In particular, with this force field both calculations predict a normal isotope effect [6], which includes a lattice contraction when H is replaced by D and a convergence of H and D volumes with increasing T, contrary to the experimental result. To complement these results, we have repeated the calculations using the polarizable TTM3-F [23,24] potential. This force field has recently been shown to outperform q-TIP4P/F when compared to experiments in PIMD simulations of $H_2{}^{18}O$ and $D_2{}^{18}O$. Results provided in Table I and in the supplementary material [20], show that this polarizable force field also fails to reproduce the anomalous isotope effect. However, as it will be discussed below, TTM3-F improves over q-TIP4P/F, displaying a stronger anticorrelation effect.

TABLE I. DFT volume (in Å^3/molecule) for proton-ordered (H-ordered) and proton-disordered (H-disordered) ice Ih for different isotopes, obtained with the quasiharmonic approximation (QHA) or path-integral (PIMD) simulations. k mesh is the effective number of $\mathbf{k}$ points for sampling the 4-molecule hexagonal Brillouin zone in the phonon calculation (one for Γ sampling). IS$(A - B) = \frac{V(A)}{V(B)} - 1$ is the relative isotope shift for the exchange of isotope A by B. The exchange and correlation (XC) functionals are PBE [25], vdW-DF$^{\text{PBE}}$ [26,27], revPBE [28], and vdW-DF$^{\text{revPBE}}$ [27]. The empirical force fields (EFF) are q-TIP4P/F [2] and TTM3-F [23]. V_{cla} is the volume for classical nuclei. Also shown are the experimental results from Ref. [12] and the ones obtained in this work. Note that they are at different temperatures.

T(K)	k-mesh	Structure	Method	XC/EFF	V_{cla}	H_2O	D_2O	$H_2{}^{18}O$	IS(H-D)	IS(^{16}O-^{18}O)
200	1	H-ordered	PIMD	PBE		31.02	31.21		−0.61%	
200	1	H-ordered	QHA	PBE	30.6	30.00	30.16	29.98	−0.53%	+0.07%
0	24	H-disordered	QHA	q-TIP4P/F	30.98	32.30	32.13	32.24	+0.53%	+0.18%
0	24	H-disordered	QHA	TTM3-F	31.66	31.67	31.67	31.67	+0.002%	+0.002%
0	24	H-disordered	QHA	PBE	29.91	29.93	30.04	29.91	−0.35%	+0.07%
0	24	H-disordered	QHA	vdW-DF$^{\text{PBE}}$	30.90	31.16	31.23	31.13	−0.23%	+0.10%
0	1	H-ordered	QHA	PBE	29.98	29.91	30.05	29.89	−0.47%	+0.07%
0	1	H-ordered	QHA	vdW-DF$^{\text{PBE}}$	30.88	31.01	31.10	30.98	−0.29%	+0.10%
0	1	H-ordered	QHA	revPBE	32.84	32.88	32.98	32.85	−0.30%	+0.09%
0	1	H-ordered	QHA	vdW-DF$^{\text{revPBE}}$	33.45	33.73	33.76	33.70	−0.09%	+0.09%
0	729	H-ordered	QHA	PBE	29.98	30.09	30.19	30.07	−0.33%	+0.07%
0	729	H-ordered	QHA	vdW-DF$^{\text{PBE}}$	30.88	31.17	31.22	31.14	−0.16%	+0.10%
0	729	H-ordered	QHA	revPBE	32.84	33.18	33.23	33.15	−0.15%	+0.09%
0	729	H-ordered	QHA	vdW-DF$^{\text{revPBE}}$	33.45	33.95	33.94	33.92	+0.03%	+0.09%
10		disordered	Exp[12]			32.054(5)	32.082(3)		−0.089(18)%	
100		disordered	Exp[12]			32.047(3)	32.072(5)		−0.079(18)%	
100		disordered	Exp (this work)			32.079(4)	32.103(4)	32.058(4)	−0.076(18)%	0.064(18)%
220		disordered	Exp[12]			32.368(4)	32.437(3)		−0.212(15)%	
220		disordered	Exp (this work)			32.367(4)	32.429(4)	32.357(4)	−0.191(17)%	0.032(17)%

Our DFT simulations are performed using the SIESTA method [29,30], with norm-conserving pseudopotentials and numerical atomic basis sets for the valence electrons. We use a basis of triple-ζ polarized orbitals, a longer and improved version of the basis set used in Ref. [26]. Given the precision needed to obtain accurate Grüneisen parameters, which involve numerical second derivatives of the forces, we have used highly converged grids for real-space and k-sampling integrations. All of our residual forces were smaller than 10^{-3} eV/Å. Details of the parameters and convergence tests are provided in the supplementary material [20].

Hexagonal ice Ih is the most common form of ice, where oxygens occupy the hexagonal wurtzite lattice sites. The two covalently-bonded protons have six possible orientations, but are constrained by Bernal-Fowler ''ice rules'' to have one proton per tetrahedral O-O bond. This structure is characterized by proton disorder [31]. Ice XI is the proton-ordered phase of ice that is formed by a transition from hexagonal ice Ih at 72 K if catalyzed by KOH^- [32]. The lattice parameters are slightly different from those of ice Ih, with the hexagonal symmetry weakly broken [33]. We have performed calculations for three crystal structures: (i) The Bernal-Fowler structure, with 12 molecules per unit cell, a net dipole moment along the c axis, and proton order consistent with the hexagonal symmetry; (ii) a version of the ordered ice XI structure with 4 molecules per unit cell, constrained to be hexagonal, also with a net dipole moment along the c axis; and (iii) a 96-molecule proton-disordered structure with no net dipole moment [6]. The oxygen lattice disorder observed in experiments [34] is of the same order of magnitude as what we observe in our PIMD simulations of the proton-disordered structure [6,35].

As the results obtained for cells (i) and (ii) are very close, in the following we will present results for structures (ii) and (iii). Table I shows the $T = 0$ volumes for several isotope combinations of H, D, ^{16}O, and ^{18}O, for all the DFT functionals [25,27,28,36] and force fields used in this study. Also included in this table is a 32 beads PIMD result for a single unit cell (Γ sampling) using the PBE-DF, compared to a calculation with the QHA for an identical system. The simulation was done at $T = 200$ K.

As the experimental study from Röttger *et al.* did not consider $H_2{}^{18}O$, we have performed high-resolution x-ray diffraction experiments of the three isotopes H_2O, D_2O, and $H_2{}^{18}O$. Results are presented in the table. Experiments were performed with samples of water frozen in thin-walled glass capillaries, open at both ends to accommodate the volume expansion upon freezing, or in flexible polymide tubes. In all cases, Si powder within the sample promoted nucleation of multiple crystals and provided an internal standard for precise determination of x-ray wavelength. X-ray measurements were performed at a temperature of 100 and 220 K K at the X16C high-resolution powder diffractometer at the National Synchrotron Light Source, using x rays of nominal wavelength 0.7 Å. Diffraction peak widths were on the order of 0.02° FWHM. Independent samples were prepared by slowly (~ 0.05 K/sec) cooling and by quenching with liquid N_2. Lattice parameters were determined from measured positions of 21 ice diffraction peaks. Reported error bars encompass selected measurements at different temperatures. A detailed experimental study including temperature dependence will be published in a future contribution.

Except for vdW-DF$^{\text{revPBE}}$, all the other XC functionals predict an anomalous isotope effect at $T = 0$ when H is replaced by D, in agreement with experiments. However, the isotope effect has the normal sign for the O atom. Our experiments confirm this result, with a 0.06% volume contraction when ^{18}O replaces ^{16}O ($T = 100$ K). The comparison of structures (ii) and (iii) shows that the results are largely independent of the ordering of the protons. Agreement with experiments improves as Brillouin zone integration is improved. With respect to their generalized gradient approximation counterparts, vdW-DFs soften the aforementioned anticorrelation effect, reducing the magnitude of the H $\rightarrow$ D isotope shift, but have little effect on the O shift. When phonons from the full Brillouin zone are accounted, the vdW-DF$^{\text{revPBE}}$ fails to predict the isotope shift at $T = 0$. However, the anomalous shift for this functional is recovered at $T > 100$ K [20]. Overall, vdW-DF$^{\text{PBE}}$ has proven to be very robust for a variety of structural and dynamical properties of water [8,27,37]. It also gives our best lattice constant for ice at $T = 0$. Therefore, in the following we use this functional and the QHA to explore the volume of ice Ih in structure (ii), including full Brillouin zone phonon integration, as a function of isotope masses and temperature. However, the results, and, in particular, the anomalous isotope effect, are very robust and largely independent of the XC functional, harmonic approximation, system size, and proton ordering.

Figure 2 shows $V(T)$ of ice Ih for standard isotope substitutions of H and O. Experimentally, the anomalous H $\rightarrow$ D isotope effect increases from 0.09% at $T = 10$ K to 0.25% at $T = 250$ K, and this increase is reproduced by our calculations (from 0.16% to 0.32%). The classical volume becomes larger than any of the quantum results above 100 K. This implies that, for larger temperatures, a classical isobaric *ab initio* molecular dynamics simulation of ice will overestimate its volume, relative to a quantum PIMD simulation.

To analyze the complex isotope-dependent free energy surface, we plot in Fig. 3 the vibrational density of states, projected onto the two atomic species, as well as the average Grüneisen constants of the different phonon branches. The volume change upon isotope substitution at $T = 0$ is approximately proportional [17,18] to the average value $\langle \omega_k \gamma_k \rangle$. Negative γ_ks imply a softening of

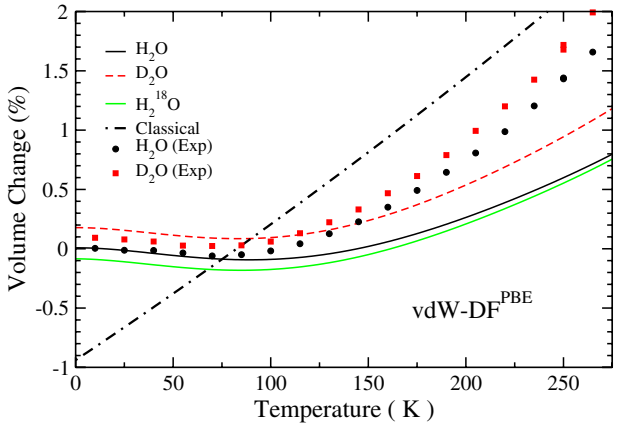

FIG. 2 (color online). Volume change $V(T)/V_{H_2O}(0) - 1$, relative to H_2O at $T = 0$, for different isotopes calculated using the QHA with the vdW-DF^{PBE} functional. Also shown are the experimental results from Ref. [12].

the modes with increasing pressure, favoring smaller volumes for lighter isotopes. Thus, the anomalous isotope effect, $V(H_2O) < V(D_2O)$, is due to the negative γ_k of the covalent OH stretching modes ($\omega \sim$ 3100–3500 cm^{-1}) which have more than 95% H weight. Although the likewise H-dominated librational modes ($\omega \sim$ 600–1000 cm^{-1}) have a positive γ_k, they are not enough to balance the volume shrinking contribution of the stretching frequencies. In the case of the TTM3-F force field, the two contributions are very small and almost completely cancel out, effectively producing a very harmonic ice crystal, with a tiny anomalous effect at high T. On the other hand, q-TIP4P/F largely underestimates the OH-O/OH anticorrelation, predicting a normal isotope effect for all temperature ranges. Long range torsional

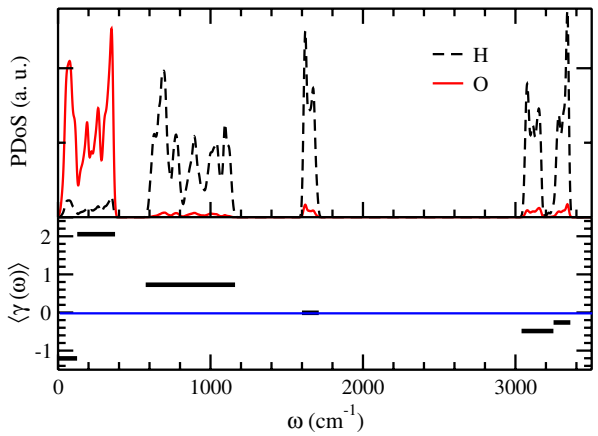

FIG. 3 (color online). Top: Density of vibrational states for H_2O, projected onto H and O atoms, for the ordered ice Ih structure, as obtained with vdW-DF^{PBE} functional. Bottom: Average Grüneisen constants of the different modes.

modes, representing rigid tetrahedral rotations with $\omega \approx$ 50 cm^{-1}, also have $\gamma_k < 0$. These modes are responsible for the negative thermal expansion below 70 K. The bending modes, with $\omega_k = 1700$ cm^{-1} and $\gamma_k \approx 0$ have little effect on volume.

Substitution of ^{16}O by ^{18}O affects mainly the low frequency modes, dominated by positive values of γ_k, producing a normal isotope effect. The temperature dependence of the isotopic O substitution is also normal, and the volume shift is 50% smaller at $T = 220$ K than at $T = 100$ K. Somewhat surprisingly, the net effect at $T = 0$, relative to classical nuclei, is dominated by quantum oxygen, resulting in a quantum volume ~1% larger. This small expansion (10 times smaller than that of Ne) is a consequence of two competing anharmonicities: the contraction effect of H-dominated stretching modes and the expansion effect of librational and translational modes. As T increases, the contribution of the stretching modes becomes dominant, causing the net quantum effect to change sign and to become anomalous above ~70 K. This dominance increases with T, making the volume shift 4 times larger at the melting temperature than at $T = 0$. These results are not inconsistent with the requirement that, at high enough T the isotope shift is isotope independent, but we find that the convergence towards the classical limit starts at $T >$ ~900 K.

Our results may also have significant implications for the understanding of nuclear quantum effects in liquid water (in which the anomalous isotope shift is experimentally larger than in ice [14]). PIMD simulations, using the q-TIP4P/F and TTM3-F EFFs, produce a less structured liquid than classical molecular-dynamic (MD) simulations [2,3,23]. However, as we have seen, these EFFs do not reproduce the anomalous isotope effect in ice, because they fail to describe accurately the derivatives of the frequencies, which govern the anharmonicities and the nuclear quantum effects in the structure and dynamics. This suggests that these models may be inadequate to reproduce some quantum effects in the liquid as well as in the solid. Therefore, the observed loss of structure in the liquid, for quantum vs classical nuclei, should be reanalyzed with an EFF that reproduces the anomalous quantum effects in ice.

In conclusion, we have shown that the anomalous nuclear quantum effects on the volume of ice can be fully understood using the quasiharmonic approximation with density-functional theory. The study fully explains a rare, seldom mentioned, property of ice which should be included in the list of water anomalies [38], as an example in which quantum effects are anomalous and increase with temperature.

We thank Christian Thomsen for suggestions at the early stage of this work. The work at Stony Brook University is supported by DOE Grants No. DE-FG02-09ER16052 (M. V. F. S) and No. DE-FG02-08ER46550 (P. B. A). Work

at Madrid is supported by Spain's MCI Grant No. FIS2009-12721-C04. Use of the National Synchrotron Light Source, Brookhaven National Laboratory, was supported by the U. S. Department of Energy, Office of Basic Energy Sciences, under Contract No. DE-AC02-98CH10886.

*maria.fernandez-serra@stonybrook.edu

[1] A. K. Soper and C. J. Benmore, Phys. Rev. Lett. **101**, 065502 (2008).
[2] S. Habershon, T. E. Markland, and D. E. Manolopoulos, J. Chem. Phys. **131**, 024501 (2009).
[3] R. Ramírez and C. P. Herrero, J. Chem. Phys. **133**, 144511 (2010).
[4] J. A. Morrone and R. Car, Phys. Rev. Lett. **101**, 017801 (2008).
[5] X.-Z. Li, B. Walker, and A. Michaelides, Proc. Natl. Acad. Sci. U.S.A. **108**, 6369 (2011).
[6] C. P. Herrero and R. Ramírez, J. Chem. Phys. **134**, 094510 (2011).
[7] A. Zeidler, P. S. Salmon, H. E. Fischer, J. C. Neuefeind, J. M. Simonson, H. Lemmel, H. Rauch, and T. E. Markland, Phys. Rev. Lett. **107**, 145501 (2011).
[8] M. V. Fernandez-Serra and E. Artacho, Phys. Rev. Lett. **96**, 016404 (2006).
[9] E. Libowitzky, Monatschefte für Chemie **130**, 1047 (1999).
[10] B. Minceva-Sukarova, W. F. Sherman, and G. R. Wilkinson, J. Phys. C **17**, 5833 (1984).
[11] F. O. Libnau, J. Toft, A. A. Christy, and O. M. Kvalheim, J. Am. Chem. Soc. **116**, 8311 (1994).
[12] K. Röttger, A. Endriss, J. Ihringer, S. Doyle, and W. F. Kuhs, Acta Crystallogr. Sect. B **50**, 644 (1994).
[13] K. Röttger, A. Endriss, J. Ihringer, S. Doyle, and W. F. Kuhs, Acta Crystallogr. Sect. B **68**, 91 (2012).
[14] G. S. Kell, J. Chem. Eng. Data **12**, 66 (1967).
[15] D. Batchelder, D. Losee, and R. Simmons, Phys. Rev. **173**, 873 (1968).
[16] C. P. Herrero, Phys. Rev. B **65**, 014112 (2001).
[17] P. B. Allen, Philos. Mag. B **70**, 527 (1994).
[18] J. M. Ziman, *Principles of the Theory of Solids* (Cambridge University Press, Cambridge, England, 1979).
[19] One can neglect thermal contributions to the electronic free energy because of the large band gap of ice.
[20] See supplemental material at http://link.aps.org/supplemental/10.1103/PhysRevLett.108.193003.
[21] T. C. Sivakumar, H. A. Chew, and G. P. Johari, Nature (London) **275**, 524 (1978).
[22] G. P. Johari, H. A. M. Chew, and T. C. Sivakumar, J. Chem. Phys. **80**, 5163 (1984).
[23] G. S. Fanourgakis and S. S. Xantheas, J. Chem. Phys. **128**, 074506 (2008).
[24] F. Paesani, S. S. Xantheas, and G. A. Voth, J. Phys. Chem. B **113**, 13118 (2009).
[25] J. P. Perdew, K. Burke, and M. Ernzerhof, Phys. Rev. Lett. **77**, 3865 (1996).
[26] J. Wang, G. Roman-Perez, J. M. Soler, E. Artacho, and M.-V. Fernandez-Serra, J. Chem. Phys. **134**, 024516 (2011).
[27] M. Dion, H. Rydberg, E. Schroder, D. C. Langreth, and B. I. Lundqvist, Phys. Rev. Lett. **92**, 246401 (2004).
[28] Y. Zhang and W. Yang, Phys. Rev. Lett. **80**, 890 (1998).
[29] P. Ordejón, E. Artacho, and J. M. Soler, Phys. Rev. B **53**, R10441 (1996).
[30] J. M. Soler, E. Artacho, J. D. Gale, A. García, J. Junquera, P. Ordejón, and D. Sanchez-Portal, J. Phys. Condens. Matter **14**, 2745 (2002).
[31] T. K. Hirsch and L. Ojamäe, J. Phys. Chem. B **108**, 15856 (2004).
[32] Y. Tajima, T. Matsuo, and H. Suga, Nature (London) **299**, 810 (1982).
[33] A. J. Leadbetter, R. C. Ward, J. W. Clark, P. A. Tucker, T. Matsuo, and H. Suga, J. Chem. Phys. **82**, 424 (1985).
[34] W. Kuhs and M. Lehmann, J. Phys. (Paris), Colloq. **48**, C1-3 (1987).
[35] It should be noted that a small amount of oxygen disorder, on the range of ± 0.008 Å is accounted for in our proton-disordered structures, and in the anisotropy of the ice XI lattice, at $T = 0$. The O atom root mean square displacement (rms) is even larger in the PIMD simulations (rms $= \pm 0.07$ Å, $T = 100$ K; ± 0.17 Å, $T = 250$ K), which include a combination of both thermal motion and extra displacements due to the anisotropy associated to the proton disorder.
[36] G. Román-Pérez and J. M. Soler, Phys. Rev. Lett. **103**, 096102 (2009).
[37] C. Zhang, J. Wu, G. Galli, and F. Gygi, J. Chem. Theory Comput. **7**, 3054 (2011).
[38] http://www.lsbu.ac.uk/water/.